

# Fabrication and Wear Resistance of $\text{TiO}_2/\text{Al}_2\text{O}_3$ Coatings by Micro-arc Oxidation

Shen Yizhou<sup>1</sup>, Tao Haijun<sup>1</sup>, Lin Yuebin<sup>1,2</sup>, Zeng Xiaofei<sup>1</sup>, Wang Tao<sup>1</sup>, Tao Jie<sup>1</sup>, Pan Lei<sup>1</sup>

<sup>1</sup> Nanjing University of Aeronautics and Astronautics, Nanjing 211100, China; <sup>2</sup> Jiangsu Provincial Key Laboratory for Interventional Medical Devices, Huaian 223003, China

**Abstract:**  $\text{TiO}_2/\text{Al}_2\text{O}_3$  composite coatings were prepared on the surface of Ti-6Al-4V alloy by micro-arc oxidation in the  $\text{Na}_2\text{SiO}_3-(\text{NaPO}_3)_6-\text{NaAlO}_2$  solution. The growth process reveals that  $\text{O}^{2-}$  reacts rapidly with  $\text{Ti}^{4+}$  (from substrate) along the reaction channels to form  $\text{TiO}_2$ , and because of the addition of  $\text{AlO}_2^-$ ,  $\text{Al}_2\text{O}_3$  and  $\text{Al}_2\text{TiO}_5$  are simultaneously formed.  $\text{Al}_2\text{TiO}_5$  is immediately decomposed into rutile  $\text{TiO}_2$  and  $\alpha\text{-Al}_2\text{O}_3$  owing to the high thermal energy caused by discharge. Finally the prepared composite phase coatings are mainly composed of anatase  $\text{TiO}_2$ , rutile  $\text{TiO}_2$  and  $\alpha\text{-Al}_2\text{O}_3$  via XRD analysis. Furthermore, the microhardness HV increases and maintains at about 11 000 MPa, and the wear resistance of the  $\text{TiO}_2/\text{Al}_2\text{O}_3$  composite coatings is enhanced by about 9.5 times than higher that of Ti-6Al-4V alloy owing to the existence of ceramic layer.

**Key words:** Ti-6Al-4V; oxidation;  $\text{TiO}_2/\text{Al}_2\text{O}_3$ ; wear

Ti-6Al-4V alloy has been widely used as a structural alloy in aerospace and biomedical fields owing to the excellent mechanical properties and corrosion resistance<sup>[1,2]</sup>. However, relatively poor tribological properties, such as high wear rate and low hardness, have hindered its further applications which require high surface hardness and wear resistance<sup>[3]</sup>. Thus, some surface modification techniques have been developed to improve the surface wear resistance of Ti-6Al-4V alloy to meet some special requirements.

At present, the methods to improve surface properties of titanium alloy mainly include thermal oxidation<sup>[4]</sup>, sol-gel method<sup>[5]</sup>, spraying and anodic oxidation<sup>[6,7]</sup>. However, the wear resistance of the coatings fabricated by the above surface modification methods is still not satisfying owing to the weak bonding strength between the coatings and substrates or the thinness.

Micro-arc oxidation (MAO) technique as a novel method of surface treatment for titanium and its alloys has been developed for many years<sup>[8]</sup>. It is derived from conventional

anodic oxidation, but different from it. Compared with anodic oxidation, MAO technique can be used to prepare much thicker and harder ceramic coatings. Furthermore, the MAO coatings have robust bonding strength with the substrate owing to the in-situ growth behavior<sup>[9]</sup>. But the wear resistance of pure  $\text{TiO}_2$  coatings prepared by micro-arc oxidation is still undesirable owing to the unstable tetragonal crystal system structure. As a kind of high wear-resistance material,  $\text{Al}_2\text{O}_3$  has been widely investigated for the applications under the harsh conditions. Thus, synthesizing the  $\text{TiO}_2/\text{Al}_2\text{O}_3$  composite coatings gradually arouse the researchers' intense interest. Up to now, only few reports illuminate the  $\text{TiO}_2/\text{Al}_2\text{O}_3$  composite coatings fabricated by micro-arc oxidation. Most researchers manufacture the composite coatings via the methods of sol-gel method and spraying<sup>[10,11]</sup>.

In the present work, the  $\text{TiO}_2/\text{Al}_2\text{O}_3$  composite coatings were prepared in the new electrolyte of  $\text{Na}_2\text{SiO}_3-(\text{NaPO}_3)_6-\text{NaAlO}_2$  by micro-arc oxidation using pulsed bipolar power

Received date: January 18, 2016

Foundation item: National Natural Science Foundation of China (51475231, 51205196, 51202112); Jiangsu Innovation Program for Graduate Education (KYLX\_0261); Fundamental Research Funds for the Central Universities

Corresponding author: Tao Jie, Professor, College of Material Science and Technology, Nanjing University of Aeronautics and Astronautics, Nanjing 211100, P. R. China, Tel: 0086-25-52112911, E-mail: taojie@nuaa.edu.cn

Copyright © 2017, Northwest Institute for Nonferrous Metal Research. Published by Elsevier BV. All rights reserved.

supply. Meanwhile, the growth process with the change of phase composition and surface morphology was investigated especially at the beginning of oxidation. Finally the wear resistance of the  $\text{TiO}_2/\text{Al}_2\text{O}_3$  composite coatings on the surface of Ti-6Al-4V alloy was also characterized and analyzed in detail.

## 1 Experiment

Ti-6Al-4V rectangular pieces (50 mm×25 mm×0.5 mm) were used as the substrate material. Subsequently, the specimens were polished with metallographic abrasive paper (60#~2000#) and cleaned ultrasonically in sequence with acetone, alcohol and distilled water for 10 min separately. Then MAO treatment was performed with constant current density of 8 A dm<sup>-2</sup>, frequency of 500 Hz and duty cycle of 20% in an aqueous solution composed of  $\text{Na}_2\text{SiO}_3$  (6 g L<sup>-1</sup>),  $(\text{NaPO}_3)_6$  (5 g L<sup>-1</sup>) and  $\text{NaAlO}_2$  (1.5 g L<sup>-1</sup>). Meanwhile, the temperature of electrolyte was kept below 40 °C by a cooling system. After oxidation, the samples were rinsed with distilled water and dried in air.

The phase composition of the MAO coatings were characterized with glancing-angle (1°) X-ray diffractometry (GAXRD; UltimaIV, Rigaku Co., Cu K $\alpha$  radiation, Japan) operating at 50 kV and 40 mA. The surface morphologies were observed by scanning electron microscope (SEM; Quanta200, FEI Co., US). The thickness of MAO coatings was tested by a thickness tester (Minitest 600d, EPK Co., Germany), and the average value of 10 measurements was calculated precisely. Surface hardness was evaluated using a micro-hardness tester (HXS-1000a, Caikon Co., China) with a load of 0.5 N for 15 s.

After MAO treatment, the wear resistance of the coatings was evaluated using a ball-on-disk friction-abrasion testing machine with an  $\Phi$  5 mm GCr15 steel ball (surface roughness  $R_a$  of 0.03  $\mu\text{m}$ , hardness of HRC 61-65) under the dry sliding conditions. The load, frequency and test time were 1.3 N, 10 Hz and 15 min, respectively. The friction coefficient was collected by the computer during each measurement.

## 2 Results and Discussion

### 2.1 Growth process of $\text{TiO}_2/\text{Al}_2\text{O}_3$ coatings

According to the experiment phenomena and theoretical analysis of micro-arc oxidation, the growth process of  $\text{TiO}_2/\text{Al}_2\text{O}_3$  composite coatings on the surface of Ti-6Al-4V alloy is established (Fig.1). At the initial stage,  $\text{O}^{2-}$  and  $\text{Al}(\text{OH})_4^-$  are produced via ionization and adsorbed to the surface of sample under the action of electric field. Subsequently,  $\text{O}^{2-}$  reacts with  $\text{Ti}^{4+}$  (from substrate) at the interface between substrate and electrolyte to form very thin and uniform  $\text{TiO}_2$  coatings. Meanwhile,  $\text{Al}_2\text{O}_3$  is also synthesized and covers the surface of as-prepared  $\text{TiO}_2$  coatings (Fig.1a, 1b).

With the increase of the voltage, there are a large number of

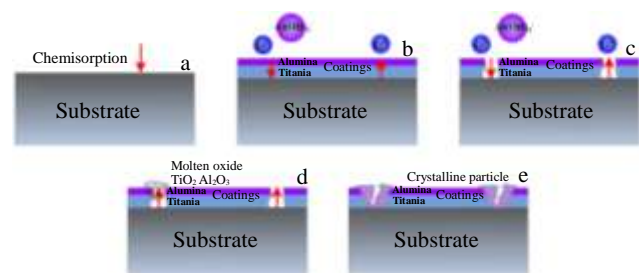


Fig.1 Growth model of  $\text{TiO}_2/\text{Al}_2\text{O}_3$  composite coatings on the surface of Ti-6Al-4V alloy

$\text{O}^{2-}$  and  $\text{Al}(\text{OH})_4^-$  being produced at the interface of coatings/electrolyte. Meanwhile the voltage has also enabled to break down the as-prepared thin  $\text{TiO}_2/\text{Al}_2\text{O}_3$  coatings to produce the ion reaction channels. Then  $\text{O}^{2-}$  and  $\text{Al}(\text{OH})_4^-$  react rapidly with  $\text{Ti}^{4+}$  along the reaction channels to form high temperature and high pressure molten oxides ( $\text{TiO}_2$ ,  $\text{Al}_2\text{O}_3$  and  $\text{Al}_2\text{TiO}_5$ ), and  $\text{Al}_2\text{TiO}_5$  is also immediately decomposed into rutile  $\text{TiO}_2$  and  $\alpha\text{-Al}_2\text{O}_3$  under the condition of the high thermal energy. At the same time, the molten oxides jet out rapidly and solidify into crystalline particles around the channels owing to liquid quenching (as shown in Fig.1c, 1e). Many electron holes appear in the coatings and drift to the cathode, which results in the enhancement of local electric field around the cathode. It is also useful to bring more plasma carriers and to cause the bigger reaction channels. The synthesized molten oxides can also continually jet out and solidify into crystalline particles. Finally the thick and uniform composite phase coatings are obtained on the surface of Ti-6Al-4V alloy<sup>[12,13]</sup>.

The change rules of the external voltage and the coating thickness during the growth process of  $\text{TiO}_2/\text{Al}_2\text{O}_3$  coatings are illustrated in Fig.2. The growth rate of the coatings is very high in the first 2 min, and starts to decrease in the subsequent period. When the oxidation time is 20 min, the thickness reaches 15.4  $\mu\text{m}$ . And it can be found that the external voltage does not increase from 10 min to 20 min and maintains at about 480 V, but the coatings continue to grow. When the thickness of coatings reaches a certain value, the coatings are very difficult to be broken down, but the relatively weak area still has disruptive discharge<sup>[14,15]</sup>. Thus, the voltage remains in a constant value, but the thickness of coatings continues to increase.

The surface morphologies of the coatings with different oxidation time are shown in Fig.3. There are few pores appearing on the surface of sample oxidized for 40 s. With the time increasing, the porous structure is clearly observed and the size of pores becomes greater and greater. When the oxidation time is 20 min, the new micro-size pores are regenerated on the pore bottom. Hence, the outermost layer of the  $\text{TiO}_2/\text{Al}_2\text{O}_3$  coatings is loose and porous. Furthermore, with the oxidation time increasing, the coatings continue to

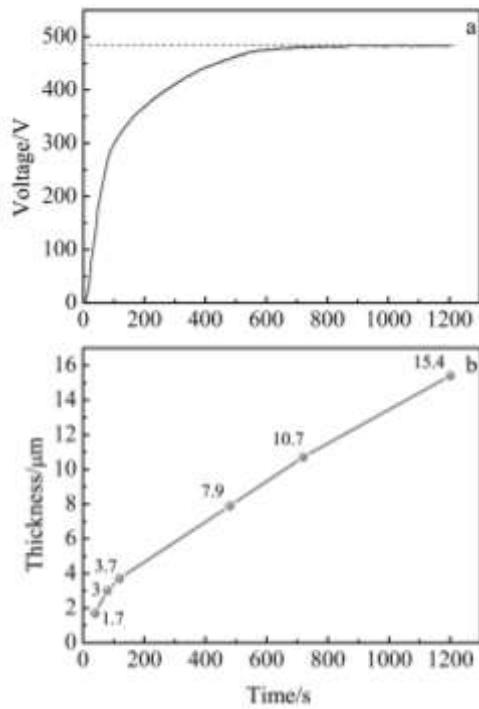


Fig.2 External voltage (a) and thickness (b) varied with the oxidation time

ceaselessly grow inside to form new oxide coatings, which can be attributed to that  $O^{2-}$  can continuously and rapidly migrate inward along the discharge channels under the condition of high temperature and strong electric field ( $10^6 \text{ V cm}^{-1}$ )<sup>[16]</sup>.

## 2.2 Section morphology of the $\text{TiO}_2/\text{Al}_2\text{O}_3$ coatings

The section morphology and main element distribution of the coatings are shown in Fig.4. Clearly, all elements (O, Al and

Ti) of the coatings are evenly distributed along the substrate, and there is no obvious discontinuity at the interfaces of the coatings/substrate, indicating high bond strengths between coatings and the Ti-6Al-4V substrate. In combination with section morphology and element distribution, the coatings can be approximately divided into three layers: the outer layer, with the highest Al content; the intermediate layer, with Al content slightly lower than that in the outer layer and maintaining at a relatively constant level; the inner layer, in which Al content is the lowest and gradually decreases to the level of the substrate.

## 2.3 Phase compositions of the coatings

It can be found in Fig.5 that the coatings are mainly composed of anatase  $\text{TiO}_2$ , rutile  $\text{TiO}_2$  and  $\alpha\text{-Al}_2\text{O}_3$ . For the composite phase MAO coatings, the intensities of these phase peaks increase gradually with the extension of oxidation time. When oxidation time is less than 8 min, the coatings are not very thick so that Ti substrate peak obviously exists in the XRD patterns.

$\text{AlO}_2^-$  ions in the electrolyte have also involved in the plasma and electrochemical reactions during the whole MAO process. Firstly,  $\text{AlO}_2^-$  ions can interact with water in the electrolyte, forming the  $\text{Al}(\text{OH})_4^-$  ions. Then, these  $\text{Al}(\text{OH})_4^-$  ions can electromigrate toward the anode surface and partly generate  $\text{Al}_2\text{O}_3$ , other  $\text{Al}(\text{OH})_4^-$  ions react with  $\text{Ti}^{4+}$  ions and  $\text{O}^{2-}$  ions to synthesize  $\text{Al}_2\text{TiO}_5$ <sup>[17]</sup>. When the temperature is about  $1280^\circ\text{C}$  (much lower than  $7700^\circ\text{C}$  caused by arc discharge),  $\text{Al}_2\text{TiO}_5$  is immediately decomposed into rutile  $\text{TiO}_2$  and  $\alpha\text{-Al}_2\text{O}_3$ . Therefore, the coatings are mainly composed of  $\text{TiO}_2$  and  $\text{Al}_2\text{O}_3$ <sup>[18-21]</sup>.

## 2.4 Wear resistance of $\text{TiO}_2/\text{Al}_2\text{O}_3$ coatings

The microhardness HV increases rapidly in the first 5 min and maintains at about 11 000 MPa from 12 min to 20 min. It is enhanced by about 1.5 times than that of the Ti-6Al-4V

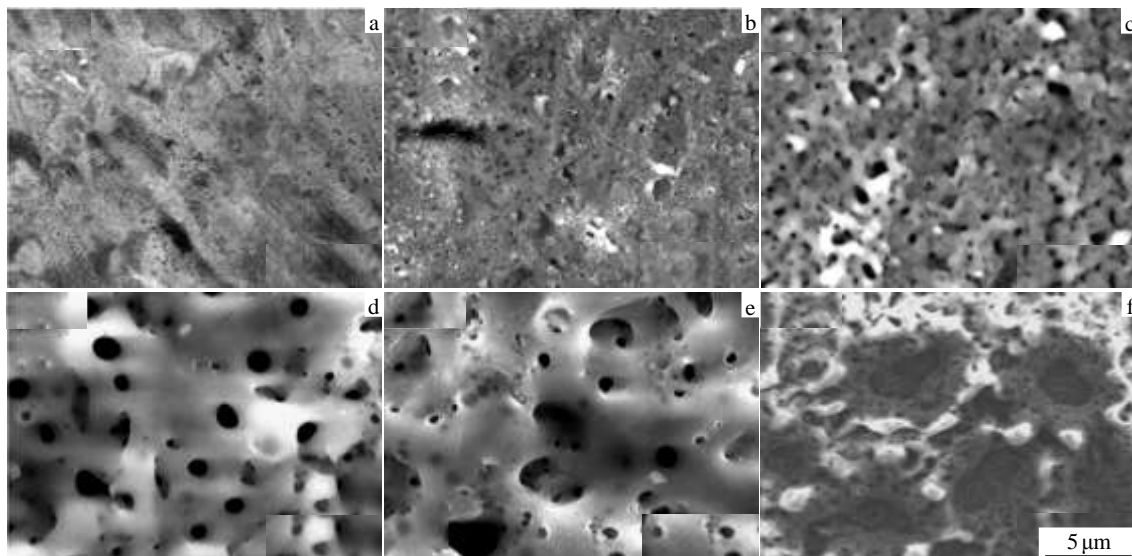


Fig.3 SEM images of  $\text{TiO}_2/\text{Al}_2\text{O}_3$  coatings with different oxidation time: (a) 40 s, (b) 80 s, (c) 2 min, (d) 8 min, (e) 12 min, and (f) 20 min

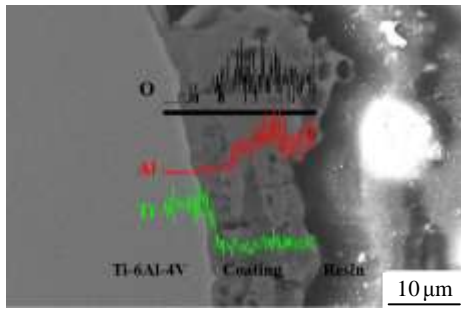


Fig.4 Section morphology and element O, Al, and Ti distribution of the coatings with oxidation time of 20 min

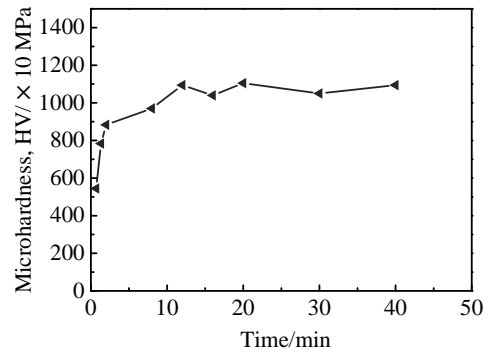


Fig.6 Effect of the oxidation time on the hardness of the TiO<sub>2</sub>/Al<sub>2</sub>O<sub>3</sub> composite coatings

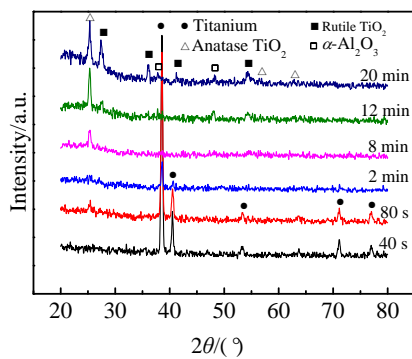


Fig.5 XRD patterns of MAO coatings with different oxidation time

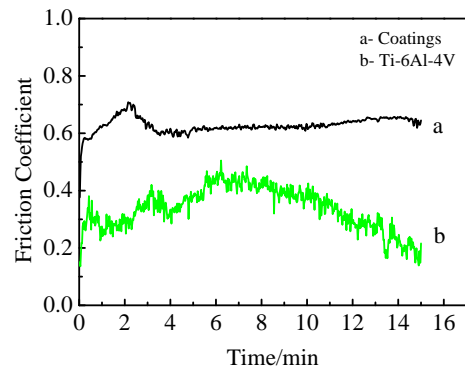


Fig.7 Friction coefficient curve of the TiO<sub>2</sub>/Al<sub>2</sub>O<sub>3</sub> composite coatings and substrate

alloy substrate (Fig.6). Subsequently, we characterized the wear resistance of the samples with the oxidation time of 20 min. The effects of wear time on friction coefficient for the coatings and Ti-6Al-4V alloy are shown in Fig.7. For the untreated substrate, the friction coefficient is about 0.4 and decreases gradually from 8 min to 15 min. However, the friction coefficient of the TiO<sub>2</sub>/Al<sub>2</sub>O<sub>3</sub> composite coatings increases rapidly in the first 2 min and declines gradually to a constant value (0.61) at later time. The wear loss of the TiO<sub>2</sub>/Al<sub>2</sub>O<sub>3</sub> composite coatings and substrate against GCr15 steel ball was also accurately measured, and the results are shown in Fig.8. The wear loss of Ti-6Al-4V alloy is about 9.5 times than that of the coatings under the same friction condition. Meanwhile, the wear trace on Ti-6Al-4V alloy is obviously deeper and wider than that on the coatings. Thus, the conclusion can be drawn that the coatings composed of anatase TiO<sub>2</sub>, rutile TiO<sub>2</sub> and α-Al<sub>2</sub>O<sub>3</sub> can greatly improve the wear resistance of the Ti-6Al-4V alloy.

The morphologies of wear trace are also obtained (seeing Fig.9) to investigate the wear resistance mechanism of the TiO<sub>2</sub>/Al<sub>2</sub>O<sub>3</sub> composite coatings. Plastic shearing occurs and many scratches and grooves appear on the wear trace of Ti-6Al-4V alloy (Fig.9a). It reveals that the wear mechanism of Ti-6Al-4V alloy against GCr15 steel ball is severe adhesive wear with a little abrasive wear<sup>[22]</sup>.

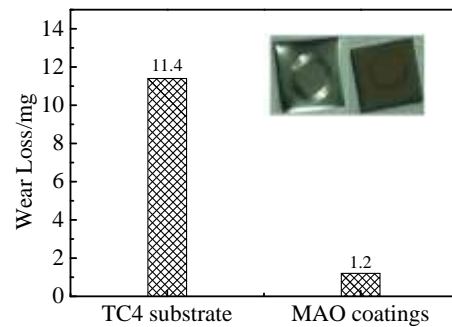


Fig.8 Wear loss of the coatings and Ti-6Al-4V alloy against GCr15 steel ball for sliding 15 min

The wear trace on the TiO<sub>2</sub>/Al<sub>2</sub>O<sub>3</sub> composite coatings reveals that the features look locally smooth (Fig.9b) because of the loose porous layer being polished away slightly. We also find that there are many small abrasive particles on the wear trace of the coatings. Meanwhile, another view can be observed that real contact area during the wear test is much smaller on the TiO<sub>2</sub>/Al<sub>2</sub>O<sub>3</sub> coatings than that on the substrate, and very slight abrasive wear also occurs between GCr15 steel ball and the coatings. It is why the wear loss of the TiO<sub>2</sub>/Al<sub>2</sub>O<sub>3</sub> composite coatings is far less than that of Ti-6Al-4V alloy.

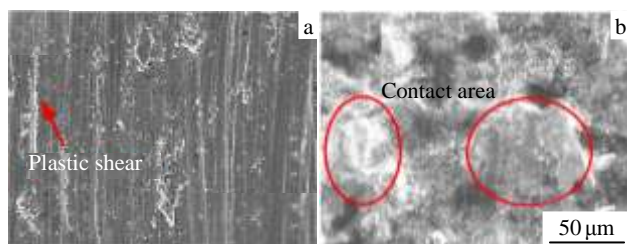


Fig.9 SEM images of wear trace for Ti-6Al-4V substrate (a) and the  $\text{TiO}_2/\text{Al}_2\text{O}_3$  composite coatings (b)

### 3 Conclusions

1) The composite phase ( $\text{TiO}_2/\text{Al}_2\text{O}_3$ ) ceramic coatings are prepared on the surface of Ti-6Al-4V alloy in the new  $\text{Na}_2\text{SiO}_3\text{-(NaPO}_3)_6\text{-NaAlO}_2$  electrolyte by micro-arc oxidation. The composite phase coatings are a typical MAO porous structure and mainly composed of anatase  $\text{TiO}_2$ , rutile  $\text{TiO}_2$  and  $\alpha\text{-Al}_2\text{O}_3$ .

2) The microhardness HV increases and maintains at about 11 000 MPa, and the wear resistance of the  $\text{TiO}_2/\text{Al}_2\text{O}_3$  composite coatings is enhanced by about 9.5 times higher than that of Ti-6Al-4V alloy. The wear resistance mechanism shows that the real contact area during the wear test is much smaller on the hard  $\text{TiO}_2/\text{Al}_2\text{O}_3$  coatings than that on the substrate and only slight abrasive wear also occurs between GCr15 steel ball and the coatings.

### References

- Sutter G, List G. *International Journal of Machine Tools and Manufacture*[J], 2013, 66: 37
- Ma T J, Chen T, Li W Y et al. *Materials Characterization*[J], 2011, 62: 130
- Atar E, Kayali E S, Cimenoglu H. *Surface and Coatings Technology*[J], 2008, 202: 4583
- Yao Z P, Shen Q X, Niu A X et al. *Surface and Coatings Technology*[J], 2014, 242: 146
- Bastami A A, Farnoush H, Sadeghi A et al. *Surface Engineering* [J], 2013, 29: 205
- Proudhon H, Savkova J, Basseville S et al. *Wear*[J], 2014, 311: 159
- Zhao Y, Xiong T Y. *Surface Engineering*[J], 2012, 28: 371
- Wen L, Wang Y M, Zhou Y et al. *Corrosion Science*[J], 2011, 53: 473
- Jin F Y, Chu P K, Wang K et al. *Materials Science and Engineering A*[J], 2008, 476: 78
- Islak S, Buytoz S, Ersöz E et al. *Optoelectronics and Advanced Materials-Rapid Communications*[J], 2012, 6: 844
- Umit Ozlem A A, Fatma Z T. *Composites Part B-Engineering*[J], 2014, 58: 147
- Zhang R F, Zhang S F. *Corrosion Science*[J], 2009, 51: 2820
- Wang Y M, Lei T Q, Jiang B L et al. *Applied Surface Science*[J], 2004, 233: 258
- Lu L H, Shen D J, Zhang J W et al. *Applied Surface Science*[J], 2011, 257: 4144
- Wang P, Li J P, Guo Y C et al. *Journal of Rare Earths*[J], 2010, 28: 798
- Wang C C, Wang F, Han Y. *Surface and Coatings Technology*[J], 2013, 214: 110
- Yan Y Y, Han Y, Li D et al. *Applied Surface Science*[J], 2010, 256: 6359
- Song E P, Ahn J, Lee S et al. *Surface and Coatings Technology* [J], 2006, 201: 1309
- Song E P, Ahn J, Lee S et al. *Surface and Coatings Technology* [J], 2008, 202: 3625
- Wang D S, Tian Z J, Shen L D et al. *Rare Metals*[J], 2009, 28: 465
- Sánchez E, Bannier E, Cantavalla V et al. *Journal of Thermal Spray Technology*[J], 2008, 17: 329
- Lin X Z, Zhu M H, Zheng J F et al. *Transactions of Nonferrous Metals Society of China*[J], 2010, 40: 537

## $\text{TiO}_2/\text{Al}_2\text{O}_3$ 微弧氧化复合涂层的制备及耐磨性研究

沈一洲<sup>1</sup>, 陶海军<sup>1</sup>, 林岳宾<sup>1,2</sup>, 曾小飞<sup>1</sup>, 汪涛<sup>1</sup>, 陶杰<sup>1</sup>, 潘蕾<sup>1</sup>

(1. 南京航空航天大学, 江苏 南京 211100)

(2. 江苏省介入医疗器械研究重点实验室, 江苏 淮安 223003)

**摘要:** 主要利用微弧氧化方法在 Ti-6Al-4V 合金表面制备  $\text{TiO}_2/\text{Al}_2\text{O}_3$  复合涂层, 并揭示了  $\text{O}^{2-}$ 、 $\text{AlO}_2^-$  和  $\text{Ti}^{4+}$  在涂层生长过程中的作用机制。在高温高电压条件下, Ti-6Al-4V 合金表面首先生成  $\text{TiO}_2$ 、 $\text{Al}_2\text{O}_3$  和  $\text{Al}_2\text{TiO}_5$ , 不断放电引起的高热能导致  $\text{Al}_2\text{TiO}_5$  进一步分解成  $\text{TiO}_2$  和  $\text{Al}_2\text{O}_3$ , 且 XRD 分析表明涂层的物相组成主要是 A- $\text{TiO}_2$ 、R- $\text{TiO}_2$  和  $\alpha\text{-Al}_2\text{O}_3$ 。耐磨性测试结果表明, 与基体相比  $\text{TiO}_2/\text{Al}_2\text{O}_3$  复合涂层的显微硬度 HV 提高到 11000 MPa, 且耐磨性显著提高, 磨损量降低了 9.5 倍。

**关键词:** Ti-6Al-4V; 微弧氧化;  $\text{TiO}_2/\text{Al}_2\text{O}_3$ ; 摩擦磨损

作者简介: 沈一洲, 男, 1988 年生, 博士, 南京航空航天大学材料科学与技术学院, 江苏 南京 211100, 电话: 025-52112911, E-mail: shenyizhou@nuaa.edu.cn